

See discussions, stats, and author profiles for this publication at: <https://www.researchgate.net/publication/282913548>

jp911663k

DATASET · OCTOBER 2015

READS

93

5 AUTHORS, INCLUDING:



[Filippo De Angelis](#)

Università degli Studi di Perugia

261 PUBLICATIONS 10,931 CITATIONS

[SEE PROFILE](#)



[Simona Fantacci](#)

Italian National Research Council

93 PUBLICATIONS 6,193 CITATIONS

[SEE PROFILE](#)



[Md Khaja Nazeeruddin](#)

École Polytechnique Fédérale de Lausanne

484 PUBLICATIONS 43,102 CITATIONS

[SEE PROFILE](#)

First-Principles Modeling of the Adsorption Geometry and Electronic Structure of Ru(II) Dyes on Extended TiO₂ Substrates for Dye-Sensitized Solar Cell Applications

Filippo De Angelis,^{*,†} Simona Fantacci,^{†,||} Annabella Selloni,[‡] Mohammad K. Nazeeruddin,[§] and Michael Grätzel[§]

Istituto CNR di Scienze e Tecnologie Molecolari (ISTM-CNR), c/o Dipartimento di Chimica, Università di Perugia, Via elce di Sotto 8, I-06213, Perugia, Italy, Department of Chemistry, Princeton University, Princeton, New Jersey 08544, and Laboratory for Photonics and Interfaces, Station 6, Institute of Chemical Sciences Engineering, School of Basic Sciences, Swiss Federal Institute of Technology, CH-1015 Lausanne, Switzerland, and Italian Institute of Technology (IIT), Center for Biomolecular Nanotechnologies, Via Barsanti, I-73010, Arnesano, Lecce, Italy

Received: December 9, 2009

We report a systematic density functional theory (DFT) computational investigation of Ru(II) sensitizer/TiO₂ systems relevant to dye-sensitized solar cells (DSSCs). Focusing on the prototypical N719 and the recently introduced YE05 sensitizers, and considering large slab and cluster models for TiO₂, we have systematically studied the influence of the molecular adsorption geometry, counterions, and surface protonation on the electronic structure of the dye/semiconductor systems by means of Car–Parrinello molecular dynamics combined with single-point hybrid functional calculations of the electronic properties. Our results show that the homoleptic N719 and YE05 dyes, both bearing two bipyridine ligands functionalized with four carboxylic groups, adsorb onto the TiO₂ surface by exploiting *three* carboxylic groups. The bulky TBA counterions employed in N719 cause a modest energy down-shift of the TiO₂ conduction band, whereas the smaller Na⁺ counterions, which can access the surface more closely, lead to a larger conduction band energy perturbation. Our results also confirm that the surface protonation plays a fundamental role in determining the DSSC efficiency, with a strong impact on both short-circuit photocurrent and open-circuit potential. Altogether, our study provides evidence that adsorption of the sensitizer via “*three anchoring sites*” is a key requisite to obtain high open-circuit potentials when employed in DSSC devices, thus paving the route to the design of new and more efficient sensitizers.

1. Introduction

Dye-sensitized solar cells (DSSCs) have attracted enormous interest in recent years as a promising approach to the direct conversion of light into electrical energy at low cost and with high efficiency.^{1–6} In these cells, sunlight is absorbed by molecular dye sensitizers on the surface of a nanostructured semiconducting TiO₂ film, to which the photoexcited electrons are subsequently transferred, while the holes are transferred to the redox electrolyte or to a hole conductor.⁷ Ruthenium(II) polypyridyl complexes have proven to be the most efficient dye sensitizers to date,⁸ particularly the tetraprotonated [*cis*-(dithiocyanato)-Ru-bis(2,2'-bipyridine-4,4'-dicarboxylate)] complex (N3) and its doubly protonated analogue (N719) (see Figure 1).^{9,10a} In these complexes, the thiocyanate ligands ensure fast regeneration of the photo-oxidized dye by the I[−]/I₃[−] redox mediator, while the two equivalent bipyridine ligands functionalized in their 4-4' positions by carboxylic groups ensure stable anchoring to the TiO₂ surface, allowing at the same time for the strong electronic coupling required for efficient excited-state charge injection.¹⁰

Despite showing only relatively intense absorptions in the blue and green spectral regions (400 and 535 nm, $\epsilon \approx 14\,000$

M^{−1} cm^{−1}),⁹ which limit to some extent the photocurrent density, the N719 dye has shown the highest open-circuit potential recorded so far in DSSCs employing the most commonly used I[−]/I₃[−] liquid electrolyte.^{10a} Record cells based on the N719 dye delivered photocurrent densities of 17.7 mA cm^{−2} and open-circuit potentials of 846 mV, which together with a good fill factor of 0.75, provided an efficiency of 11.2%.^{10a} (The overall conversion efficiency of DSSCs, $\eta = (i_{ph})(V_{oc})(ff)/I_s$, is determined by the product of the photocurrent density (i_{ph}), the open-circuit potential (V_{oc}), and the fill factor (ff) of the cell, normalized to the intensity of the incident light (I_s).) The efficiencies of N719-based DSSCs were also found to depend significantly on detailed features of the sensitizer such as the number of protons carried by the anchoring groups, which can thus be tuned to obtain maximum performance.^{10a,11}

Recently developed heteroleptic dyes, in which one of the 2,2'-bipyridine-4,4'-dicarboxylate ligands of N719 is specifically functionalized to obtain increased light-harvesting and red spectral response, showed photocurrent densities as high as 19.7–21.6 mA cm^{−2} when employed in DSSC devices.^{12,13} Obviously, if one could conjugate the high open-circuit potential obtained with the N719 dye to the high photocurrent densities achieved by heteroleptic dyes, breakthrough DSSC efficiencies exceeding 13% could be obtained. Quite unexpectedly, however, experiments showed that the open-circuit potential of DSSCs employing such heteroleptic dyes is significantly lower compared to that observed using the parent N719 dye, lying usually below 750 mV.^{12–16} In particular, a series of homogeneous

* Corresponding author. E-mail: filippo@chc.unipg.it.

† ISTM-CNR, Perugia.

‡ Princeton University.

§ Swiss Federal Institute of Technology.

|| Italian Institute of Technology.

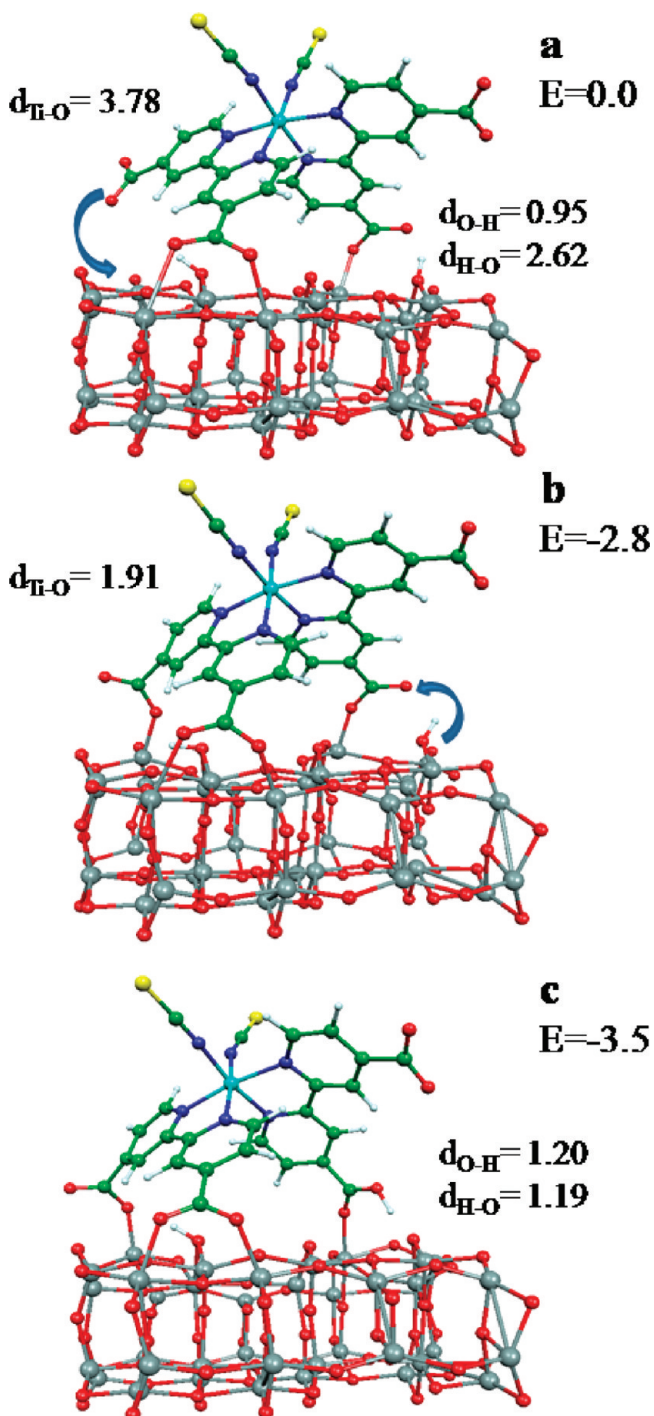


Figure 1. Representative structures of the N719 dye adsorbed on the (TiO₂)₃₈ slab model obtained during the CP molecular dynamics simulation described in the text. The relative energies of the optimized structures (kcal/mol) are also reported. (a) Starting optimized structure with the dye binding to TiO₂ via two carboxylic groups and two protons on the surface. (b) Intermediate structure where a third carboxylic group is bound to the surface. (c) Final structure in which a proton is shared between the surface and a monocoordinated carboxylic group. Distances in Å.

DSSCs fabricated under the same conditions and with the same TiO₂ paste/electrolyte formulation, but employing N719 or heteroleptic dyes,^{17a} showed a consistently reduced open-circuit potential for cells employing the latter dyes, pointing at a precise dye effect in determining the cell open-circuit potential.

First-principles calculations carried out to understand these findings showed that the sensitizers dipole can induce a shift in

the TiO₂ conduction band which in turn leads to a reduced open-circuit potential in DSSCs employing heteroleptic dyes.¹⁷ A similar dipole effect on the DSSCs open-circuit potential was also found with coadsorbing species.¹⁸ On the other hand, a possible reason of the high open-circuit potential obtained with the N719 dye may be that the (two to four) carboxylic groups in contact with the TiO₂ semiconductor surface charge it negatively, thus shifting the TiO₂ conduction band to higher energy. Another possibility is that, due to its adsorption geometry, N719 could form a denser monolayer on the TiO₂ surface, compared to heteroleptic dyes. This property may reduce the recombination of TiO₂-injected electrons with the oxidized electrolyte by preventing the I₃⁻ anions to approach the semiconductor surface, thus further enhancing the open-circuit potential (recombination reduces the electron density into the titania, thus lowering the device Fermi level). In fact, whereas N719 can adsorb onto TiO₂ by exploiting up to four carboxylic groups, heteroleptic dyes, with only one 4'-4'-carboxy-bipyridine, can exploit no more than two carboxylic groups for anchoring.¹⁷ The relevance of the anchoring mode on the photovoltaic performances of Ru(II) dyes is also supported by a recent study,¹⁹ in which a new dye with two equivalent bipyridines and a phenyl-pyridine cyclometalated ligand replacing the thiocyanate ligands (hereafter YE05) was found to deliver a DSSC open-circuit potential of ~800 mV, close to the value of ~850 mV characteristic of highly optimized N719-based DSSCs.¹⁹

Altogether, the above observations provide evidence that the N719 dye adsorption mode onto TiO₂ is a key ingredient to its success. The important question is then: what is the adsorption structure of N719 (and of the related YE05 dye) on TiO₂ and what are the implications of this unique adsorption geometry on the DSSC efficiency? On the basis of the N3 dye and the crystal structure of TiO₂ anatase, Shklover et al. proposed that the dye binds to TiO₂ through two carboxylic groups.²⁰ Combining Raman and IR spectra, Finnie et al.²¹ concluded that the N3 dye is attached to TiO₂ by a bidentate or chelate bridging mode, involving also a fraction of uncoordinated carboxylic groups. Attenuated total reflection Fourier transform infrared (ATR-FTIR) measurements by Nazeeruddin et al. provided additional insight into the dye adsorption mode,¹¹ showing a major component arising from the deprotonated carboxylic groups and a smaller component related to protonated carboxylic groups. A bidentate or bridging coordination mode has also been proposed by Pérez-León et al. on the basis of Raman and FTIR spectroscopies.²² Resonance Raman spectroscopy has also been widely employed to gauge the adsorption mode of Ru(II) dyes on titania²³ and the dye/titania/electrolyte interactions in DSSCs.²⁴ Despite these efforts, however, no conclusive assignment of the specific adsorption geometry has been achieved so far.

In this paper we present density functional theory (DFT)-based molecular dynamics simulations and electronic structure calculations aimed at establishing the detailed adsorption geometry of the N719 and YE05 dyes on TiO₂. To this end we consider extended TiO₂ models and systematically investigate the effect of the dye counterions, surface protonation, as well as solvation, on the electronic structure of the adsorbed dyes on TiO₂. These extended models and the employed high-level computational setup represent so far the most advanced and realistic simulations of DSSC devices and allow us to gain unprecedented insights into the detailed factors governing their efficiency.

2. Models and Computational Details

To model the TiO_2 nanoparticles and surfaces, we considered $(\text{TiO}_2)_{38}^{25-27}$ and $(\text{TiO}_2)_{82}$ clusters, see Supporting Information, both obtained by appropriately “cutting” an anatase slab exposing the majority (101) surface.²⁸ The larger $(\text{TiO}_2)_{82}$ model is an almost square TiO_2 (101) surface slab of ~ 2 nm side, with three rows of five- and six-coordinated surface Ti sites, which is large enough to avoid possible spurious dye/titania interactions due to the finite cluster size. The smaller $(\text{TiO}_2)_{38}$ cluster, basically a part of the $(\text{TiO}_2)_{82}$ slab, represents a good trade-off between accuracy and computational convenience and nicely reproduces the main electronic characteristics of TiO_2 nanoparticles.²⁶ The smaller model was thus employed for computationally intensive ab initio molecular dynamics simulations based on the Car–Parrinello (CP) method,²⁹ using the PBE exchange-correlation functional³⁰ together with a plane wave basis set and ultrasoft pseudopotentials.³¹ Selected configurations generated during the CP dynamics simulation were then optimized, again by the CP method, using the larger $(\text{TiO}_2)_{82}$ model. These optimizations were followed by single-point electronic structure calculations employing the hybrid B3LYP functional³² and including the effect of the surrounding water solvent, using 3-21G* and DZVP basis sets³³ in conjunction with a polarizable continuum model of solvation (C-PCM),³⁴ as implemented in the Gaussian03 program package.³⁵ The calculations explicitly included also the dye counterions, either the real tetrabutyl ammonium (TBA) or Na^+ counterions carried by the N719 dye. Both geometry optimization and electronic structure analyses were performed by selectively including one or two protons in the considered model.

To validate our computational approach, we carried out time dependent-DFT (TDDFT) single-point B3LYP calculations in solution on the CP-optimized $(\text{TiO}_2)_{82}$ cluster, see below. For the adsorbate-free cluster, we obtained a lowest excitation energy of 3.67 eV, which, added to the highest occupied molecular orbital (HOMO) energy of -7.55 eV, gives a conduction band energy estimate of -3.88 eV versus vacuum, -0.56 eV versus NHE, in good agreement with experimental band gaps³⁶ and conduction band edges estimated from flat band potentials.⁴ These results are also consistent with our previous calculations for the $(\text{TiO}_2)_{38}$ cluster,³⁷ confirming the adequacy of the present models for describing the DSSC’s electronic properties, in particular the alignment of the dye/semiconductor energy levels.³⁷

3. Results and Discussion

3.1. Adsorption of N719 and YE05 on Titania.

Recently, we investigated the electronic and optical properties of the $(\text{TiO}_2)_{38}$ cluster sensitized by the N719 dye,^{17a,38} considering the limiting cases in which the two protons carried by the dye were either retained on the dye or transferred to the TiO_2 surface. We found the latter situation to be largely favored energetically,³⁸ in agreement with previous results by Persson and Lundqvist who studied the N3 dye bound to the same $(\text{TiO}_2)_{38}$ cluster via two carboxylic groups residing on the same bipyridine.³⁹ However, due the limited dimensions of the investigated TiO_2 model and the partial or local nature of the geometry optimizations, those studies do not allow to reach clear conclusions concerning the dye adsorption mode.

To search for energetically more favorable structures on the complex potential energy surface of the adsorbed dye/ TiO_2 system, in the present study we performed CP molecular dynamics simulations starting from the N719/ $(\text{TiO}_2)_{38}$ configuration with two protons on the TiO_2 surface, Figure 1. The

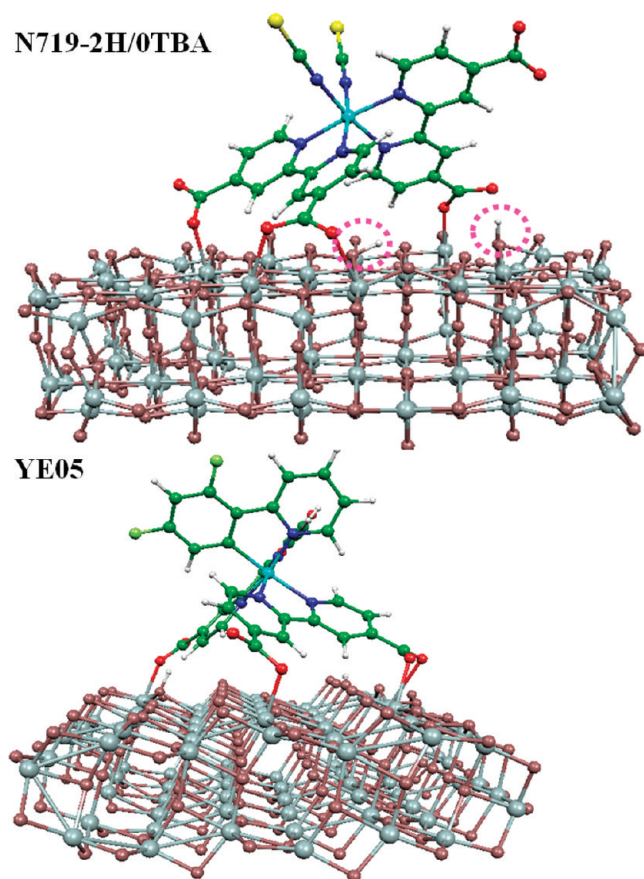


Figure 2. Upper panel: optimized geometrical structure of the N719 dye with two protons and no counterions (N719–2H/0TBA) adsorbed on the $(\text{TiO}_2)_{82}$ extended model. The dotted circles denote the positions of the two protons. Lower panel: optimized structure of the related YE05–2H/0TBA dye on the $(\text{TiO}_2)_{82}$ cluster. Notice the different orientation compared to the N719 structure.

simulation was carried out at $T \sim 400$ K for a duration of 2 ps in order to sample the configuration space around the local minimum corresponding to the starting structure. A few relevant structures generated during the simulation are reported in Figure 1, while a movie showing the system evolution in time is presented as Supporting Information. Upon heating the optimized configuration in which N719 is adsorbed on TiO_2 via two carboxylic groups and two protons reside on the surface (structure a in Figure 1), a third carboxylic group coordinates to an unsaturated Ti(IV) center of the (101) anatase surface (structure b in Figure 1). This is clearly indicated by the shortening of the corresponding Ti–O distance from 3.78 to 1.91 Å, a value characteristic of the formation of a chemical bond. Although this involved a rather small energy gain (2.8 kcal/mol after geometry optimization) the third carboxylic group remained attached to TiO_2 throughout the rest of the simulation, 1.6 ps, suggesting a strong interaction between the negatively charged carboxylic group and the unsaturated Ti(IV) center. After about 1 ps, one of the two surface-bound protons starts to interact with the free oxygen of a nearby monodentate carboxylic group and is finally shared by this oxygen on the carboxylic group and the titania surface (structure c in Figure 1). These results suggest that dye binding through *three* carboxylic groups to the TiO_2 surface is energetically and sterically feasible, with protons residing mainly on the surface but undergoing some dynamical exchange with the carboxylic groups on the molecule. Indeed, the energy gain from structure b to structure c is only 0.7 kcal/mol, i.e., comparable to room

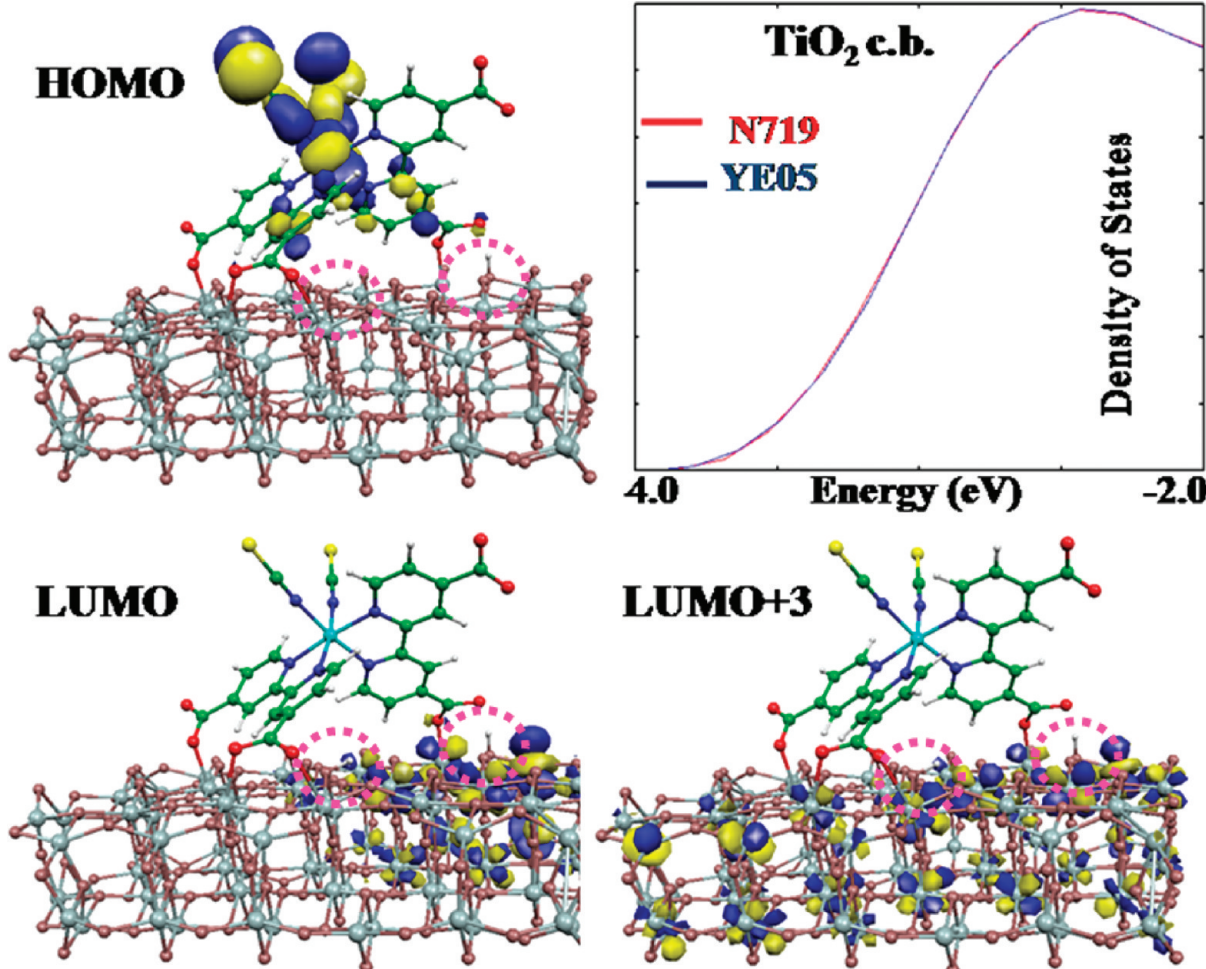


Figure 3. Isodensity plots of the LUMO and LUMO + 3 orbitals of the N719–2H/0TBA system. The dotted circles denote the positions of the two protons. Right panel: density of states in the region of the TiO₂ conduction band for analogous N719 (red line) and YE05 (blue line) systems. Notice that the two lines are almost indistinguishable.

temperature (RT) (0.59 kcal/mol at 298 K). Obviously these results might be sensitive to the surface hydration and to its detailed topological features, as well as to the pH of the electrolyte solution. Nevertheless our model highlights some salient features of the dye/surface interactions which could play a relevant role in DSSC devices.

To gain clearer insights into the interactions between the dye and the semiconductor surface, we expanded the (TiO₂)₃₈ model, where the cluster boundaries can play a significant role, and docked the final dye structure obtained from the CP simulations onto the larger (TiO₂)₈₂ cluster. This was followed by geometry optimization of the extended model. We hereafter label the investigated N719 and YE05 systems by the number of protons (xH), and number and nature ($yTBA$ or yNa) of counterions. The resulting structure shown in Figure 2 (referred to as N719–2H/0TBA) confirms that dye binding occurs via *three* carboxylic groups. As we discuss below, this has profound consequences on the electronic structure of dye-sensitized titania. We further point out, that the three anchoring sites adsorption of N719 and YE05 should also increase the system stability toward dye desorption compared, e.g., to heteroleptic dyes with only two anchoring groups, a highly desirable requisite for practical DSSC applications and long-term device durability.

Of the three carboxylic groups involved in the binding of N719–2H/0TBA to TiO₂, one is attached to two surface Ti atoms in a bidentate mode, while the other two are bound in a monodentate mode. The optimized structure also confirms that

TiO₂ protonation is energetically favorable: one proton is firmly bound to a surface oxygen close to the bidentate-bound carboxylic group (O–H distance 1.02 Å), while the other proton is bound to a surface oxygen (O–H distance 1.06 Å), hydrogen-bonding the uncoordinated oxygen of the monodentate carboxylic group, see Figure 2, upper panel. Concerning the protons location, we investigated various structures in which one of the two protons was selectively displaced, but all these other possibilities turned out to be of higher energy.

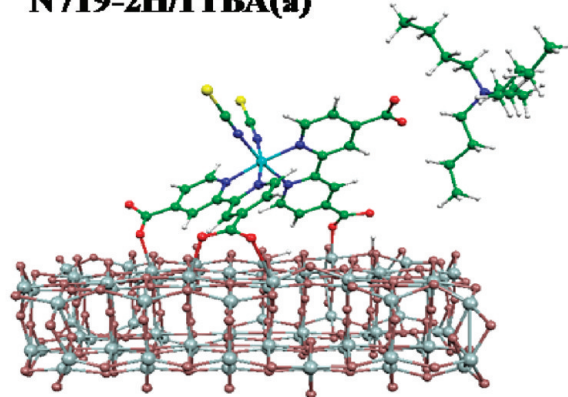
Inspection of the electronic structure of the N719–2H/0TBA system reveals the expected dye/semiconductor alignment of the energy levels, with mixed Ru–NCS HOMOs (Figure 3) inserting within the TiO₂ band gap,^{39,40} and the dye π^* orbitals overlapping with the TiO₂ conduction band. As found previously,^{11,38} the surface protonation has important implications for the DSSC efficiency, since it gives rise to an increased dye/semiconductor coupling, most likely corresponding to a higher photocurrent, at the expenses of a TiO₂ conduction band energy down-shift which reduces the open-circuit potential. Here we further notice that the spatial localization of the lowest unoccupied TiO₂ states is also affected by protonation of the surface: the lowest unoccupied molecular orbital (LUMO), Figure 3, and the LUMO + 1/LUMO + 2 (not shown) of the N719-A system are indeed TiO₂ unoccupied states localized close to the point where the proton shared by the monocoordinated carboxylic group and the surface is located, whereas the LUMO + 3, Figure 3, is a delocalized state but with an important contribution from

the Ti atoms close to the two protons. This suggests that the surface protons act as “funnels” for the dye excited electrons, ensuring a strong coupling between the dye excited states and the TiO_2 unoccupied states. The localization of the LUMO TiO_2 state near the proton shared by the monocoordinated carboxylic group and the surface is possibly due to the fact that there the proton positive charge is only partially screened by donation from the monocoordinated carboxylic group to TiO_2 , whereas in the case of bidentate carboxylic coordination a larger screening of the proton positive charge is achieved, which results in a more delocalized state.

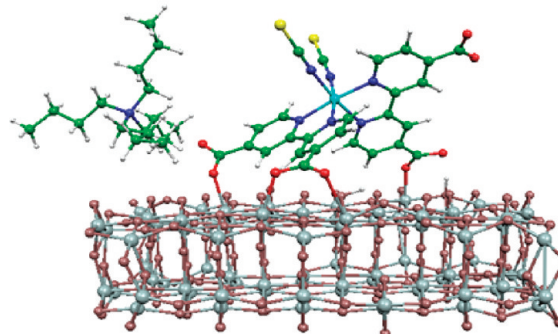
To further explore whether the high open-circuit potentials observed experimentally in DSSCs employing the N719 and YE05 dyes^{10,19} is indeed related to the adsorption geometry with “three anchoring sites”, we optimized also the structure of the YE05–2H/0TBA dye starting from the geometry optimized for the related N719 system. As expected, we found relatively minor differences in the adsorption geometries of the two dyes, Figure 2. Most notably, despite the different total charges of the two systems (−2 and −1 for N719 and YE05, respectively), their conduction bands appear to be practically identical over a wide energy range, see total density of states in Figure 3. This result is consistent with the high open-circuit potentials exhibited by both dyes and suggests that the adsorption through three anchoring sites is essential for such high performances. The residual difference in open-circuit potential between the two dyes (~50 mV) might be due to a slightly different proton content in N719 and YE05.¹⁹ Notice that in Figure 3 and in the following, Figure 6, we consider the density of states derived from the Kohn–Sham eigenvalues rather than performing TDDFT excited-state calculations. This is due to reasons of computational cost, as TDDFT calculations for the present system would require a very large number of excited states to span a reasonably wide energy interval above the lowest excited state. Our simplified procedure is further justified by the fact that we are mainly interested in relative shifts of the energy levels rather than at quantitatively reproducing the excitation energies of these very large systems.

3.2. Role of Counterions in N719. Another important issue concerns the role of counterions in fine-tuning the photovoltaic properties of the N719 dye. The native N719 dye is prepared with two protons and two TBA counterions saturating the dye doubly negative charge.¹⁰ It was found by high-resolution mass spectrometry measurements⁴¹ that in the solution conditions used for dyeing the nanostructured titania electrode in DSSC devices one of the two TBA counterions is solvated so that the main species present in solution is the diprotonated N719 monoanion forming an ion-pair with one TBA (N719–2H/1TBA).⁴¹ When the dye is adsorbed onto the TiO_2 surface, this TBA counterion can either interact with a surface-bound carboxylic group or bind to the only uncoordinated carboxylic group, configurations N719–2H/1TBA(a) and N719–2H/1TBA(b), respectively, in Figure 4. In the experiment of ref 41, however, two minor peaks were also observed, one ascribed to the diprotonated dye with no counterions, corresponding to our optimized N719–2H/0TBA structure of Figure 2, and the other to a monoprotonated species with both TBA counterions, N719–1H/2TBA in Figure 4. Since it is not known how and to what extent the ion-pairing between the dye and the counterions affects the electronic properties of dye-sensitized TiO_2 , we have decided to examine all the three systems that are observed experimentally. For the sake of completeness, we also simulated the neutral species with two protons and two TBA counterions, N719–2H/2TBA, and

N719–2H/1TBA(a)



N719–2H/1TBA(b)



N719–1H/2TBA

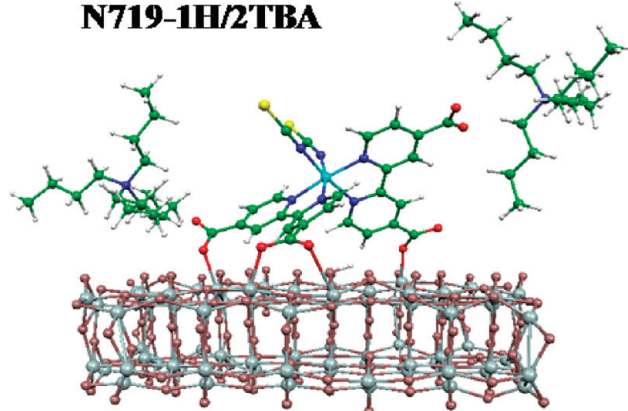


Figure 4. Optimized geometrical structures of the N719–2H/1TBA(a), –2H/1TBA(b), and –1H/2TBA systems, containing, respectively, two protons and one TBA counterion in different positions, and one proton and two TBA counterions. N719–2H/1TBA(b) is calculated to be more stable than N719–2H/1TBA(a) by 6.8 kcal/mol.

the corresponding species in which the TBA counterions have been replaced by Na^+ , N719–2H/2Na, Figure 5.

To illustrate how the number (zero, one, or two) and nature (TBA^+ or Na^+) of the counterions as well as the number or surface protons (one or two) affect the electronic structure of the investigated systems, in Figure 6 we report the density of unoccupied states for the relevant N719-based systems. Inspection of the upper panel of Figure 6 shows that the presence of two TBA counterions (red curve) leads to a slight energy down-shift (ca. 0.03 eV) of the TiO_2 conduction band peak.

Such a small effect is due to the fact that even for the closest $\text{TBA}-\text{TiO}_2$ contact (e.g., in the left side of N719–2H/2TBA in Figure 5) the positively charged TBA ammonium is quite far away from the semiconductor surface. Replacement of TBA with Na counterions has instead a more significant effect, as the energy down-shift of the TiO_2 conduction band is in this

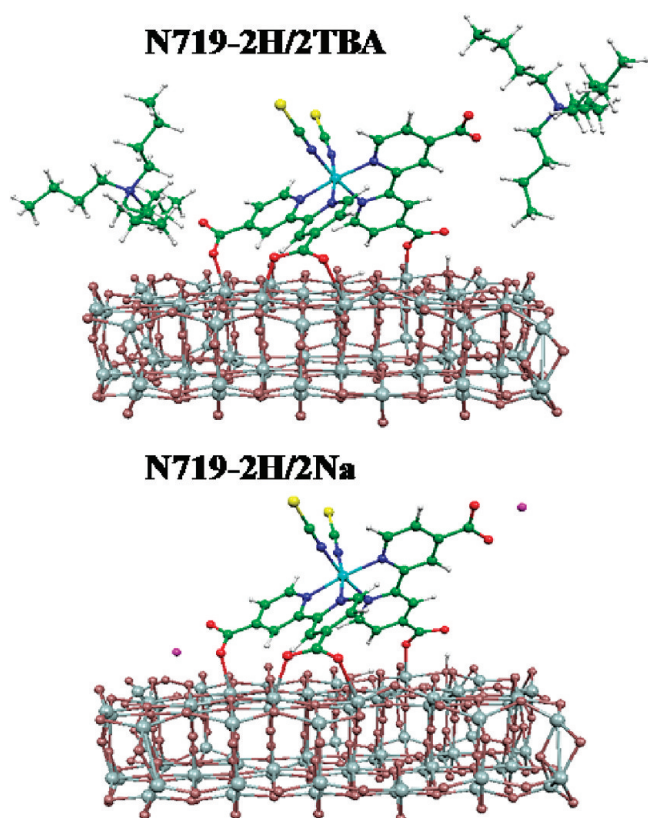


Figure 5. Optimized geometrical structures of the N719-2H/2TBA and -2H/2Na systems; see also the caption of Figure 4. Notice the Na ions in magenta close to two carboxylic groups.

case ca. 0.07 eV, see Figure 6. This is due to the fact that the smaller Na⁺ cations can access the TiO₂ surface more closely, with a consequent polarization effect that stabilizes the conduction band energy. Interestingly, the effect of counterions for a fixed number of protons (two in this case) is mostly exerted on the main conduction band peak, whereas the conduction band edge is affected to a lower extent, see inset of Figure 6, upper panel. The systems with only one TBA counterion (N719-2H/1TBA(a) and -2H/1TBA(b), Figure 4) show a conduction band shape and position similar to that with N719-2H/2TBA, as expected considering the limited effect (at most 0.03 eV) of TBA counterions discussed above. Notice, however, that the configuration with the TBA counterion close to the titania surface (N719-2H/1TBA(b)) is predicted to be significantly more stable than N719-2H/1TBA(a), see caption of Figure 4, suggesting that in the experimental conditions used in DSSC fabrication, the dominant monoanionic diprotonated N719 species with one TBA counterion is adsorbed onto TiO₂ together with one TBA counterion close to the surface. This is in agreement with results of combined thermogravimetric, NMR, and FT-IR analyses performed on N719 adsorbed onto TiO₂,⁴² which unambiguously showed that the Ru(II) dye is grafted on titania along with *one* coadsorbed TBA counterion.

In the lower panel of Figure 6 we report the calculated density of unoccupied states for the systems with two TBA counterions but bearing two (N719-2H/2TBA) or one (N719-1H/2TBA) protons on the TiO₂ surface. As previously observed, changing the surface protonation has a profound effect on the position of the TiO₂ conduction band.³⁸ In the present case we find an upward shift of ca. 0.10 eV upon decreasing the proton content from two to one. As a matter of fact, the position of the titania conduction band follows indeed a Nernstian behavior, with a 0.059 V energy down-shift per pH unit.⁴³ What is also interesting

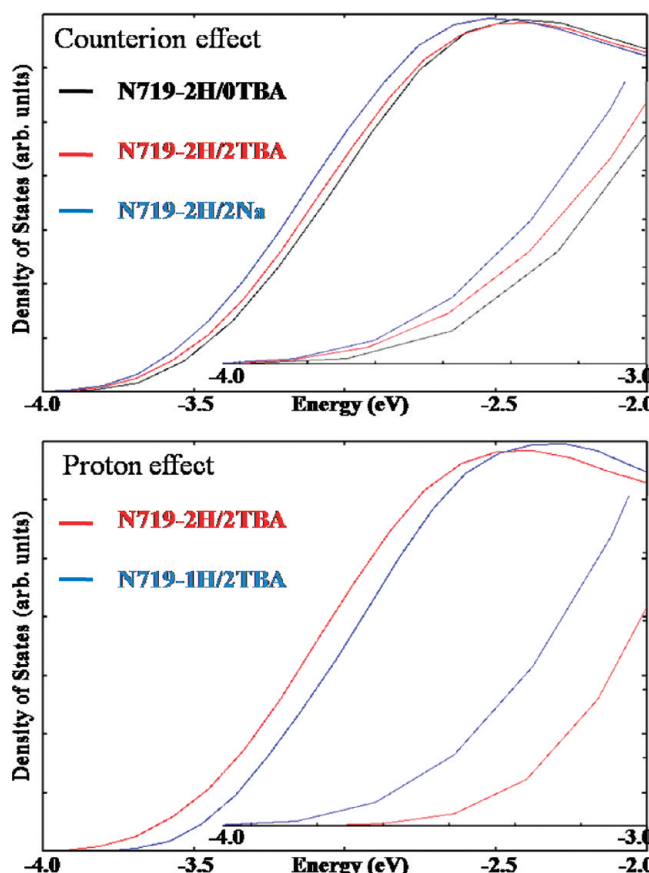


Figure 6. Upper panel: density of states in the region of the TiO₂ conduction band for N719-2H/0TBA (black line), N719-2H/2TBA (red line), and N719-1H/2Na (blue line), highlighting the effect of counterions. Lower panel: density of states in the region of the TiO₂ conduction band for N719-2H/2TBA (red line) and N719-1H/2TBA (blue line), highlighting the effect of surface protonation. The insets show a magnification of the energy region close to the TiO₂ conduction band edge.

to notice here is that the energy shift associated with TiO₂ protonation involves both the edge and the main peak of the conduction band, at variance with the counterion effect. This suggests that the surface protonation might affect both the open-circuit potential *and* the electron injection close to the edge and high in the conduction band. Both effects have indeed been observed, and their optimization allowed us to obtain the 11.2% DSSC efficiency reported in ref 10.

4. Concluding Remarks

We have reported a DFT study of the structure and electronic properties of the prototypical N719 and YE05 Ru(II) sensitizers adsorbed on extended TiO₂ models, by combining CP molecular dynamics simulations and geometry optimizations with single-point hybrid functional electronic structure calculations in solution. Our high-level computational approach allows us to gain unprecedented insight into the nature of the dye/semiconductor heterointerface and thus into the detailed factors ultimately governing DSSCs efficiency.

We have shown that the N719 and YE05 dyes, both bearing two bipyridine ligands functionalized with four carboxylic groups, adsorb onto the TiO₂ surface by exploiting *three* carboxylic groups. The two protons initially carried by the N719 dye are transferred to the semiconductor surface, even though one of the two protons is actually shared between the dye and a nearby TiO₂ surface oxygen. The related YE05 dye is found

to exhibit the same adsorption geometry as N719. Inspection of the electronic structure for the N719- and YE05-sensitized systems shows an almost identical TiO_2 conduction band energy and shape, suggesting that the high open-circuit potential observed in DSSCs employing the two sensitizers can be related to their adsorption geometry. As a matter of fact, DSSCs based on heteroleptic sensitizers, which can only exploit two carboxylic group for grating onto TiO_2 , constantly exhibit lower open-circuit potentials. This turns out to be due to a number of factors, including the favorable sensitizer dipole, the increased charge donation from the three anchoring carboxylates to the TiO_2 , and possibly the formation of a more compact dye layer, which reduces parasitic recombination reactions, in comparison to heteroleptic dyes. Moreover, the adsorption via three anchoring sites should provide additional stability toward dye desorption, a highly desirable requisite for practical DSSC applications and long-term device durability.

A further reason for the high open-circuit potential delivered by N719 is related to the choice of appropriate counterions. Indeed, the bulky TBA counterions employed experimentally cause a modest (within 0.01–0.03 eV) energy down-shift of the TiO_2 conduction band, whereas smaller counterions such as Na^+ , which can easily access the surface, would lead to a larger conduction band energy down-shift of 0.07 eV.

Our calculations also confirm the important influence of surface protonation on the DSSC open-circuit potential, with a conduction band energy down-shift of as much as 0.1 eV when varying the number of surface protons from one to two. The surface-bound protons induce a strong localization of unoccupied TiO_2 states in the neighborhood of the proton positions, these states acting as funnels for the photoexcited electrons, thus substantially increasing the electronic coupling and leading to the higher photocurrents observed experimentally. Although the main effect of the counterions is to cause an energy shift of the high-lying TiO_2 conduction band states, surface protonation affects also the conduction band edge, in line with the strong open-circuit potential variation observed upon changing the sensitizer's proton content.

In conclusion, our results allow us to identify the sensitizer “three anchoring sites” as a fundamental requisite to obtain high open-circuit potentials when employed in DSSC devices, thus paving the route to the design of new sensitizers coupling this efficient anchoring mode with the introduction of highly absorbing moieties aimed at increasing the light-harvesting capability of the dyes.

Acknowledgment. F.D.A. and S.F. thank Fondazione Istituto Italiano di Tecnologia - Project SEED 2009 (HELYOS) for financial support. A.S. acknowledges support from the U.S. Department of Energy (Grant DE-FG02-05ER15702). MKN thanks WCU (World Class University) program through the National Research Foundation of Korea funded by the Ministry of Education, Science and Technology, Grant No. R31-10035.

Supporting Information Available: Optimized geometrical structures of the $(\text{TiO}_2)_{38}$ and $(\text{TiO}_2)_{82}$ systems, full ref 35, and a movie file showing the adsorption dynamics. This material is available free of charge via the Internet at <http://pubs.acs.org>.

References and Notes

- O'Regan, B.; Grätzel, M. *Nature* **1991**, 353, 737.
- Rehm, J. M.; McLendon, G. L.; Nagasawa, Y.; Yoshihara, K.; Moser, J.; Grätzel, M. *J. Phys. Chem. B* **1996**, 100, 9577.
- Hagfeldt, A.; Grätzel, M. *Chem. Rev.* **1995**, 95, 49.
- Grätzel, M. *Nature* **2001**, 414, 338–344.
- Nazeeruddin, M. K.; Wang, Q.; Cevey, L.; Aranyos, V.; Liska, P.; Figgemeier, E.; Klein, C.; Hirata, N.; Koops, S.; Haque, S. A.; Durrant, J. R.; Hagfeldt, A.; Lever, A. B. P.; Grätzel, M. *Inorg. Chem.* **2006**, 45, 787.
- Kamat, P. V. *J. Phys. Chem. C* **2007**, 111, 2834.
- Nazeeruddin, M. K.; Grätzel, M. In *Molecular and Supramolecular Photochemistry*; Ramamurthy, V., Schanze, K. S., Eds.; Marcel Dekker: New York, 2003; Vol. 10, p 301.
- Grätzel, M. *C. R. Chim.* **2006**, 9, 578.
- Nazeeruddin, M. K.; Kay, A.; Rodicio, I.; Humphry-Baker, R.; Muller, E.; Liska, P.; Vlachopoulos, N.; Grätzel, M. *J. Am. Chem. Soc.* **1993**, 115, 6382.
- (a) Nazeeruddin, M. K.; De Angelis, F.; Fantacci, S.; Selloni, A.; Viscardi, G.; Liska, P.; Ito, S.; Takeru, B.; Grätzel, M. *J. Am. Chem. Soc.* **2005**, 127, 16835. (b) Fantacci, S.; De Angelis, F.; Selloni, A. *J. Am. Chem. Soc.* **2003**, 125, 4381.
- Nazeeruddin, M. K.; Humphry-Baker, R.; Liska, P.; Grätzel, M. *J. Phys. Chem. B* **2003**, 107, 8981.
- Abbotto, A.; Barolo, C.; Bellotto, L.; Angelis, F. D.; Grätzel, M.; Manfredi, N.; Marinzi, C.; Fantacci, S.; Yum, J.-H.; Nazeeruddin, M. K. *Chem. Commun.* **2008**, 42, 5318.
- Chen, C.-Y.; Wu, S.-J.; Li, J.-Y.; Wu, C.-G.; Chen, J.-G.; Ho, K.-C. *Adv. Mater.* **2007**, 19, 3888.
- Nazeeruddin, M. K.; Bessho, T.; Cevey, L.; Ito, S.; Klein, C.; De Angelis, F.; Fantacci, S.; Comte, P.; Liska, P.; Imai, H.; Grätzel, M. *J. Photochem. Photobiol. A* **2007**, 185, 331.
- Nazeeruddin, M. K.; Zakeeruddin, S. K.; Lagref, J.-J.; Barolo, C.; Viscardi, G.; Liska, P.; Comte, P.; Schenk, K.; Grätzel, M. *Coord. Chem. Rev.* **2004**, 248, 1317.
- Wang, P.; Klein, C.; Humphry-Baker, R.; Zakeeruddin, S. M.; Grätzel, M. *J. Am. Chem. Soc.* **2004**, 126, 808.
- (a) De Angelis, F.; Fantacci, S.; Selloni, A.; Grätzel, M.; Nazeeruddin, M. K. *Nano Lett.* **2007**, 7, 3189. (b) Chen, P.; Yum, J.-H.; De Angelis, F.; Mosconi, E.; Fantacci, S.; Moon, J.-J.; Humphry Baker, R.; Ko, J.; Nazeeruddin, M. K.; Grätzel, M. *Nano Lett.* **2009**, 9, 2487.
- Rühle, S.; Greenshtein, M.; Chen, S.-G.; Merson, A.; Pizem, H.; Sukenik, C. S.; Cahen, D.; Zaban, A. *J. Phys. Chem. B* **2005**, 109, 18907.
- Bessho, T.; Yoneda, E.; Yum, J.-H.; Guglielmi, M.; Tavernelli, I.; Imai, H.; Rothlisberger, U.; Nazeeruddin, M. K.; Grätzel, M. *J. Am. Chem. Soc.* **2009**, 131, 5930.
- Shklover, V.; Ovchinnikov, Y.-E.; Braginsky, L. S.; Zakeruddin, S. M.; Grätzel, M. *Chem. Mater.* **1998**, 10, 2533.
- Finnie, K. S.; Bartlett, J. R.; Woolfrey, J. L. *Langmuir* **1998**, 14, 2744.
- Pérez-León, C.; Kador, L.; Peng, B.; Thelakkat, K. *J. Phys. Chem. B* **2006**, 110, 8723.
- (a) Umapathy, S.; Cartner, A. M.; Parker, A. W.; Hester, R. E. *J. Phys. Chem.* **1990**, 94, 8880. (b) Meyer, T. J.; Meyer, G. G.; Pfennig, B. W.; Schoonover, J. R.; Timpson, C. J.; Wall, J. F.; Kobush, C.; Chen, X.; Peek, B. M.; Wall, C. G.; Ou, W.; Erickson, B. W.; Bignozzi, C. A. *Inorg. Chem.* **1994**, 33, 3952. (c) Shoultz, L. C. T.; Loppnow, G. R. *J. Am. Chem. Soc.* **2003**, 125, 15636. (d) Stergiopoulos, T.; Ghicov, A.; Likodimos, V.; Tsoukerlis, D. S.; Kunze, J.; Schmuki, P.; Falaras, P. *Nanotechnology* **2008**, 19, 235602.
- (a) Greijer, H.; Lidgren, J.; Hagfeldt, A. *J. Phys. Chem. B* **2001**, 105, 6314. (b) Greijer, H.; Lidgren, J.; Hagfeldt, A. *J. Photophys. Photobiol. A* **2004**, 164, 23.
- Persson, P.; Bergstrom, R.; Lunell, S. *J. Phys. Chem. B* **2000**, 104, 10348.
- De Angelis, F.; Tilocca, A.; Selloni, A. *J. Am. Chem. Soc.* **2004**, 126, 15024.
- Lundqvist, M. J.; Nilsing, M.; Lunell, S.; Akemark, B.; Persson, P. *J. Phys. Chem. B* **2006**, 110, 20513.
- Vittadini, A.; Selloni, A.; Rotzinger, F. P.; Grätzel, M. *Phys. Rev. Lett.* **1998**, 81, 2954.
- Car, R.; Parrinello, M. *Phys. Rev. Lett.* **1985**, 55, 2471.
- Perdew, J. P.; Burke, K.; Ernzerhof, M. *Phys. Rev. Lett.* **1996**, 77, 3865.
- (a) Pasquarello, A.; Laasonen, K.; Car, R.; Lee, C.; Vanderbilt, D. *Phys. Rev. Lett.* **1992**, 69, 1982–1985. (b) Giannozzi, P.; De Angelis, F.; Car, R. *J. Chem. Phys.* **2004**, 120, 5903.
- Becke, A. D. *J. Chem. Phys.* **1993**, 98, 5648.
- Godbout, N.; Salahub, D. R.; Andzelm, J.; Wimmer, E. *Can. J. Chem.* **1980**, 102, 939.
- (a) Cossi, M.; Barone, V. *J. Chem. Phys.* **2001**, 115, 4708. (b) Cossi, M.; Rega, N.; Scalmani, G.; Barone, V. *J. Comput. Chem.* **2003**, 24, 669.
- Frisch, M. J.; et al. Gaussian 03, revision B.05; Gaussian, Inc.: Pittsburgh, PA, 2003.
- (a) Weng, Y. X.; Wang, Y. Q.; Asbury, J. B.; Ghosh, H. N.; Lian, T. *J. Phys. Chem. B* **2000**, 104, 93. (b) Khoudiakov, M.; Parise, A. R.; Brunschwig, B. S. *J. Am. Chem. Soc.* **2003**, 125, 4637.

- (37) De Angelis, F.; Fantacci, S.; Selloni, A. *Nanotechnology* **2008**, *19*, 424002.
- (38) De Angelis, F.; Fantacci, S.; Selloni, A.; Nazeeruddin, M. K.; Grätzel, M. *J. Am. Chem. Soc.* **2007**, *129*, 14156.
- (39) Persson, P.; Lundqvist, M. *J. Phys. Chem. B* **2005**, *109*, 1191.
- (40) Rensmo, H.; Södergren, S.; Patthey, L.; Westmark, K.; Vayssières, L.; Khole, O.; Brühwiler, P. A.; Hagfeldt, A.; Siegbahn, H. *Chem. Phys. Lett.* **1997**, *274*, 51.
- (41) Buscaino, R.; Baiocchi, C.; Barolo, C.; Medana, C.; Grätzel, M.; Nazeeruddin, M. K.; Viscardi, G. *Inorg. Chim. Acta* **2008**, *361*, 798.
- (42) Nazeeruddin, M. K.; Amirnasr, M.; Comte, P.; Mackay, J. R.; McQuillan, A. J.; Houriet, R.; Grätzel, M. *Langmuir* **2000**, *16*, 8525.
- (43) Kalyanasundaram, K.; Grätzel, M. *Coord. Chem. Rev.* **1998**, *77*, 347.

JP911663K